

Reduced Graphene Oxide/Polydopamine/Gold Electrode as Electrochemical Sensor for Simultaneous Determination of Ascorbic Acid, Dopamine, and Uric Acid

Ling Shi^{1,2}, Zefeng Wang^{1,2,*}, Xianlan Chen^{1,2}, Guangming Yang^{1,2,*}, Wei Liu^{1,2}

¹ School of science, Honghe University, mengzi, Yunnan 661199, PR China

² Key Laboratory of Natural Pharmaceutical & Chemical Biology of Yunnan Province, Mengzi, Yunnan 661199, PR China

*E-mail: wangzefeng841006@163.com, yangguangmingbs@126.com

Received: 28 May 2019 / Accepted: 5 July 2019 / Published: 31 July 2019

In this paper, the reduced graphene oxide/polydopamine (RGO/PDA) nanocomposites are obtained *via* the reduction of GO nanosheets by dopamine, followed by simultaneous modify by PDA. Then Au nanoparticles (NPs) decorated RGO/PDA (RGO/PDA/Au) nanocatalyst was synthesized *via* in situ reduction. The obtained RGO/PDA/Au nanocatalyst is analyzed by transmission electron microscopy (TEM) and electrochemical measurements. It is found that RGO/PDA/Au nanocatalyst exhibits good electrochemical catalytic activity can be detect AA, DA and UA individual and simultaneous. The detection limit of AA, DA and UA are 1.64 mM, 0.11 mM, 0.13 mM, respectively. The prepared RGO/PDA/Au nanocatalyst possesses a large surface area, unique biocompatibility and excellent conductivity will benefit for the electrocatalytic oxidation of AA, DA and UA.

Keywords: Polydopamine, Reduced graphene oxide, Au nanoparticles, Ascorbic acid, Dopamine, Uric acid

1. INTRODUCTION

Clinical research has found that Dopamine (DA), ascorbic acid (AA), and uric acid (UA) coexist in human body. These substances play an important role in human life activities. The amount of these substances in the body has crucial effect on human health [1, 2, 3]. For example, the overdose of DA will result Schizophrenia and Parkinson's disease [4]. Irregular levels of UA may result hyperuricemia, pneumonia and gout [5]. So simultaneous determination of AA, DA, and UA have an obvious significance for human health. Recently, a variety of methods have been used to detect AA, DA, and UA. The electrochemical method has been used widely because of its simple, high sensitivity, and low cost. However, DA, AA, and UA are coexisted in the human body and the oxidation peaks

potentials of three analytes are similar. So, it remains enormous challenges whether can simultaneous detect three analytes.

Nanomaterials have been extensively employed as electrode material in electrochemical sensor. Graphene is considered to be a highly-studied carbon allotrope, owing to its excellent electrical conductivity, large surface area and chemical stability [6]. Recently, graphene based derivatives can be obtained through the incorporation of various kinds of functional materials. The potential application of graphene-based materials for electrochemical sensor has attracted much attention. Polydopamine (PDA) can adsorb onto the surface of graphene due to the PDA contains abundant positively charged sites. PDA modified graphene can effectively prevent graphene from aggregating [7]. PDA can be obtained through self-polymerization of dopamine at weak alkaline pH [8]. Zhou et al reported that PDA can be aligned magnetic nanoparticles through self-polymerization of PDA [9]. Ruan et al reported a new PDA-GOD-GN biosensor and the fabricated sensor shows good selectivity, high response sensitivity and stability [10]. Ren et al prepared that stable dispersion of PDA-modified RGO composites can be used as a good substrate material for loading metal NPs [11].

In this paper, Au nanoparticles decorated on RGO/PDA were prepared *via* in situ reduction method. The prepared nanocatalyst was characterized by X-ray diffraction (XRD) and transmission electron microscopy (TEM). Then the RGO/PDA/Au was used to assemble the electrochemical sensor for the simultaneous determination of AA, DA and UA. The as-prepared sensor shows simultaneous detection of AA, DA, and UA. Also, there is good peak separation between peaks due to the excellent electrocatalytic properties of the RGO/PDA/Au nanocatalyst.

2. EXPERIMENTAL

2.1 Materials

Graphite powder and dopamine hydrochloride (98%) were purchased from Alfa Aesar. Uric Acid (>99 %), ascorbic acid (>99 %), HAuCl₄ (99.99%, wt.%), and NaBH₄ were received from Shanghai Chemical Reagent Co. Ltd (Shanghai, China). Other chemicals used in this experiment were of analytical grade and were used without further purification. Ultra-pure water was obtained with a Milli-Q plus water purification system (Millipore Co. Ltd., USA) (18 M).

2.2 Apparatus

The RGO/PDA/Au nanohybrids were characterized by transmission electron microscope (TEM, JEM-2100). The crystal structure of the products was analyzed by a X'Pert³ powder diffractometer (PANalytical Company).

Cyclic voltammogram (CV) and differential pulse voltammogram (DPV) measurements were performed on a CHI 660E electrochemical analyzer (CHI, Shanghai). A three-electrode setup was employed, a bare glassy carbon electrode (GCE, 3 mm diameter), a Ag/AgCl electrode and a platinum wire electrode.

2.3 Preparation of RGO/PDA hybrid nanocomposites

Graphene oxide (GO) was obtained by oxidation of natural graphite powder according to a Hummers method [12, 13]. The PDA decorated reduced GO (RGO) were prepared by our reported method before [14]. 60 mg GO was dispersed in 80 mL of ultra-pure water by ultrasonication. 40 mg of dopamine hydrochloride was put into the above GO dispersion. The obtained solutions were ultrasonicated for 30 min at room ambient. Then the pH of obtained suspension solutions was adjusted to weak alkaline by adding 40 mL Tris-HCl solution (12.5 mM, pH =8.5). Meantime, the self-polymerization of dopamine was induced with vigorous stirring at 80°C and the reaction was keep for 24 h. The obtained mixture was centrifuged, washed with ultra-pure water.

2.4 Preparation of Au nanoparticles decorated on RGO/PDA nanohybrids

0.5 mL of 20 mg mL⁻¹ HAuCl₄ solution and 14.705 mg of trisodium citrate were added into 20 mL of 0.5 mg mL⁻¹ RGO/PDA hybrid nanocomposites aqueous suspension. And then the obtained solutions were vigorously stirred for 6 h to increase the interaction of Au³⁺ with RGO/PDA surface. Then, 0.6 mL of 0.1 mol L⁻¹ fresh ice-cold NaBH₄ solution was slowly added into above mixture [11]. Finally, the resulted solutions were centrifuged, washed with ethanol and ultra-pure water.

3. RESULT AND DISCUSSION

3.1 Characterization

The morphology of the RGO/PDA/Au nanocatalyst was characterized by TEM. The TEM image of the nanocatalyst is shown in Figure 1, the Au NPs with certain aggregation disperse evenly on the surface of RGO/PDA. RGO/PDA nanocomposites in RGO/PDA/Au nanohybrid seem to be lamellar and transparent morphology.

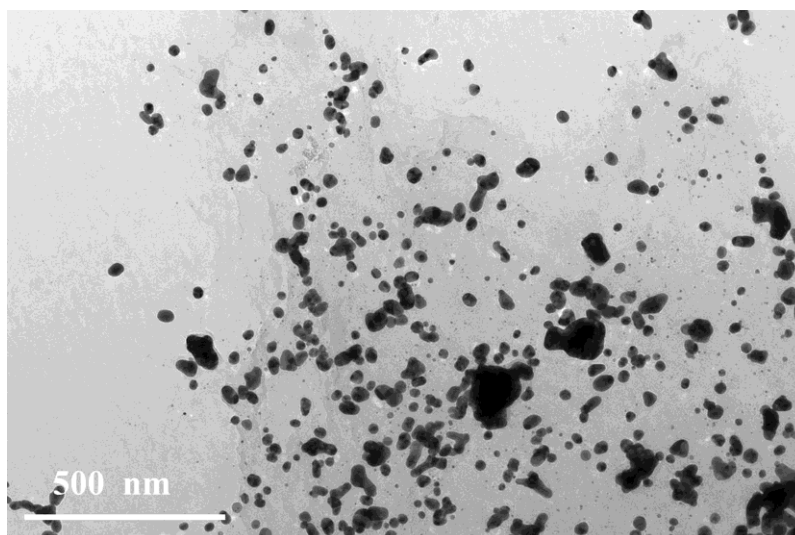


Figure 1. TEM images of RGO/PDA/Au nanohybrids.

The crystalline structures of the RGO/PDA/Au nanohybrids were determined by XRD analysis, as shown in Figure 2. The RGO/PDA nanocomposites show a wide diffraction peak at $2\theta=26.8^\circ$, corresponding to the (002) plane of RGO [15]. The pattern of RGO/PDA/Au nanocatalyst showed diffraction peaks at $2\theta=38.2^\circ$, 44.6° , 64.8° , 77.7° and 81.9° , which are related to the (111), (200), (220), (311) and (222) of lattice planes of Au NPs [16]. The results further indicate the successful formation of RGO/PDA/Au nanohybrids.

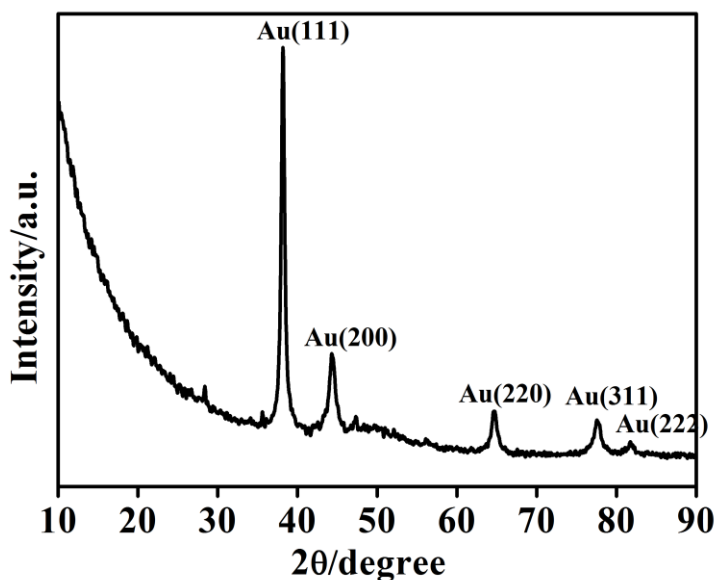


Figure 2. XRD patterns of RGO/PDA/Au nanohybrids

CV is the effective and convenient technique for probing the electronic transfer program of the modified electrode [17]. As shown in Figure 3A, the RGO/GCE shows two very broad redox peaks (curve a). The RGO/PDA/GCE (Figure 3A, curve b) exhibits larger peak current response than the RGO modified GCE. The peak current of RGO/PDA/GCE is about 2.4 times of RGO/GCE. That may be due to the RGO/PDA nanocomposites can effectively increase the conductivity of electrode to accelerate the electron-transfer. When RGO/PDA/Au nanocatalyst modified on the electrode, an increased redox peaks current (Figure 3A, curve c) is obtained. That will be due to the Au NPs possess excellent conductivity, large specific surface area, and biocompatibility.

An electrochemical impedance spectroscopy (EIS) is used to characterize the electrochemical impedance changes of different modified electrodes at the electrode surface [18]. As shown in Figure 3B, Nyquist plots of three modified electrodes in 1.0 mM $[\text{Fe}(\text{CN})_6]^{4-/3-}$ solution. The electron transfer resistance (R_{ct}) values for RGO/GCE (curve a), RGO/PDA/GCE (curve b), and RGO/PDA/Au/GCE (curve c) are 384.6 Ω , 376.6 Ω , and 200.6 Ω , respectively. There was a significant decrease in the R_{ct} value after the Au NPs decorated RGO/PDA nanocomposite, indicating enhanced electron transfer occurring at the RGO/PDA/Au/GCE.

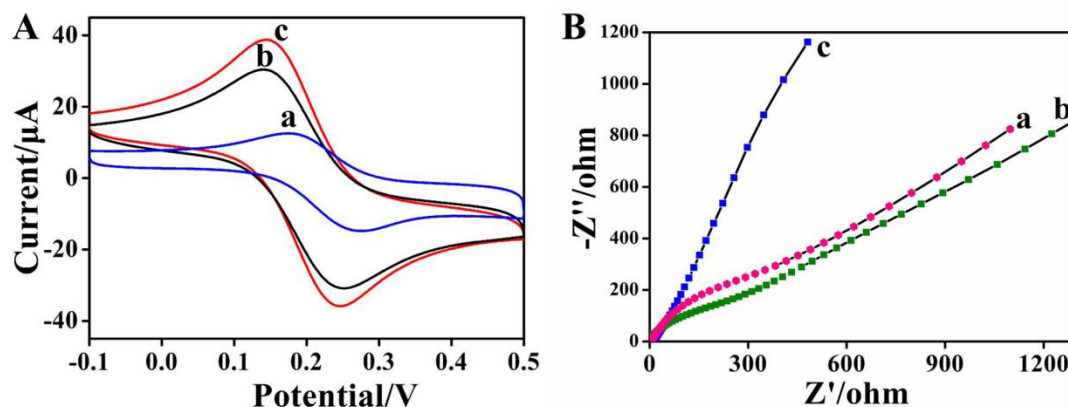


Figure 3. CVs (A) and EIS spectrums (B) of RGO/GCE (curve a), RGO/PDA/GCE (curve b), and RGO/PDA/Au/GCE (curve c). All measurements were processed in 1.0 mM $[\text{Fe}(\text{CN})_6]^{4-/3-}$ containing 0.1 M KCl.

3.2 Electrochemical behaviors of AA, DA and UA on modified electrodes

CVs of AA, DA and UA on different nanomaterials modified electrodes were recorded in Figure 4A. For bare electrode, the oxidation peaks of AA and DA are overlapped seriously (curve a). Also the oxidation peaks are wide and close on RGO modified electrode (curve b). The oxidation peak of AA was indistinguishable indicating the infeasibility of the simultaneous determination of AA, DA, UA at RGO/PDA/GCE (curve c). However, for the RGO/PDA/Au/GCE, the oxidation peaks of AA, DA and UA are well separated and a higher current appeared compared with RGO/PDA/GCE, RGO/GCE and bare GCE. The oxidation peaks of AA, DA and UA located at -0.01, 0.15 and 0.27 V, respectively. The three oxidation peaks are well separated. Furthermore, a remarkable increase in each peak current was observed at the RGO/PDA/Au modified GCE. This fact shows that the simultaneous determination of AA, DA, and UA could be achieved at RGO/PDA/Au/GCE. The reasons may be due to the synergic effect of RGO, PDA and Au NPs to facilitate the discrimination of AA, DA, and UA, the modified electrode displayed excellent catalytic activity and selectivity toward the oxidation of AA, DA, and UA [19, 20]. Figure 4B shows the DPV response of RGO/PDA/Au modified electrode in PBS containing 1.43 mM AA, 0.07 mM DA and 0.29 mM UA. Three oxidation peaks of AA, DA and UA located at -0.04, 0.13 and 0.25 V can be observed. The peak separations for AA-DA are 0.17 V, DA-UA are 0.12 V, respectively. The results further prove that simultaneous determination of AA, DA, and UA can be achieved at RGO/PDA/Au/GCE.

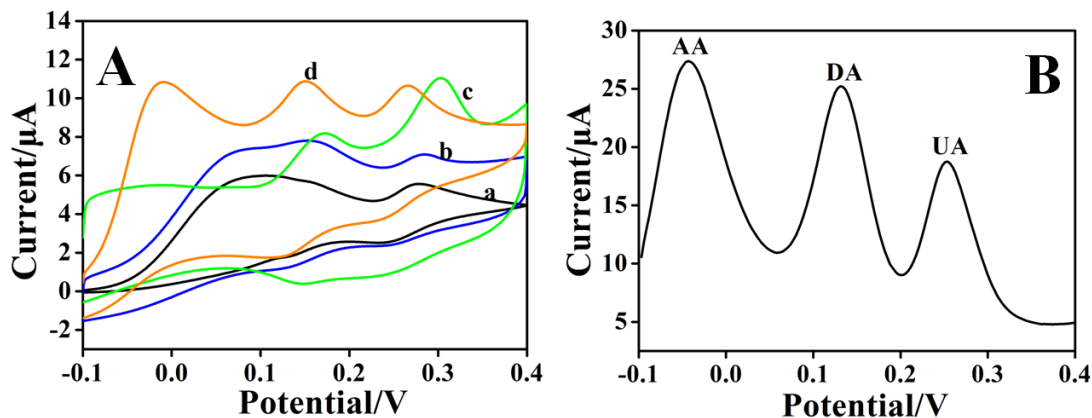


Figure 4. (A) CVs of the bare GCE (curve a), RGO/GCE (curve b), RGO/PDA/GCE (curve c) and RGO/PDA/Au/GCE (curve d) in 0.2 M PBS (pH 7.0) containing 1.43 mM AA, 0.07 mM DA and 0.29 mM UA. Scan rate is 5 mV/s; (B) DPV of RGO/PDA/Au/GCE in 0.2 M PBS (pH=7.0) containing 1.43 mM AA, 0.07 mM DA and 0.29 mM UA.

3.3 Effect of scan rate

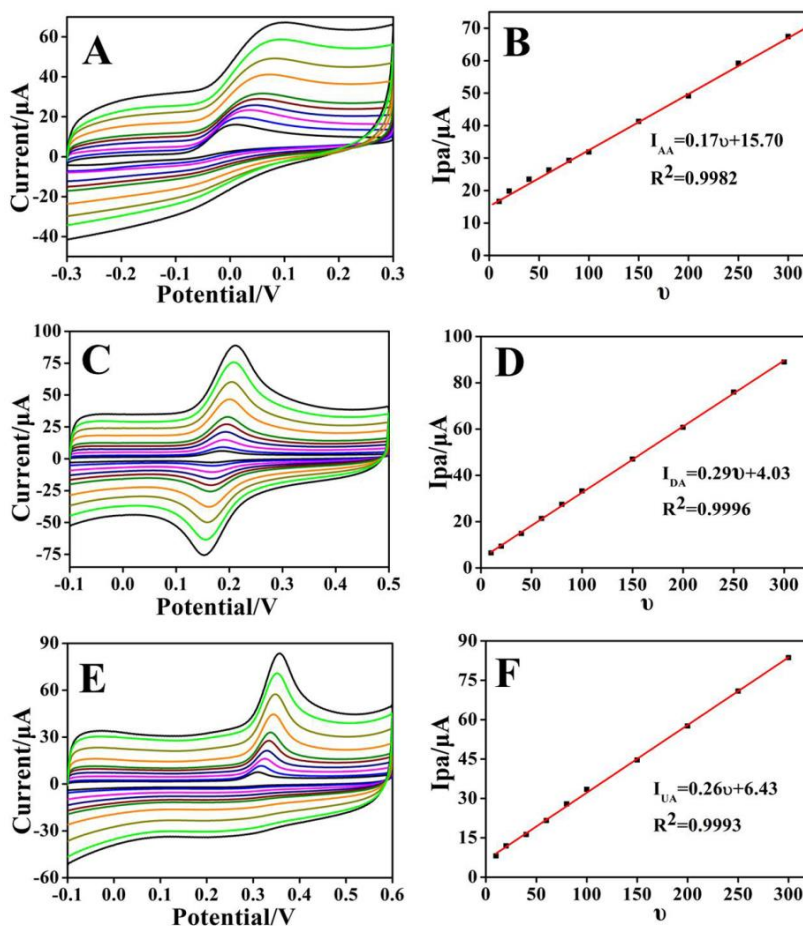


Figure 5. Effect of the scan rate on the cyclic voltammetric response of 2.86 mM AA (A), 0.14 mM DA (B), and 0.29 mM UA (C) at the RGO/PDA/Au/GCE at 10, 20, 40, 60, 80, 100, 150, 200, 250, 300 mV/s.

Figure 5 reveals the CV responses of 2.86 mM AA, 0.14 mM DA and 0.29 mM UA at RGO/PDA/Au/GCE with different scan rates from 10 to 300 mV/s. With the increase of scan rates, redox peak currents increase at the same time. The linear equations of AA, DA and UA (Figure 5B, D, F) can be described as: $I_{AA}=0.17v+15.70$ ($R^2=0.9982$), $I_{DA}=0.29v+4.03$ ($R^2=0.9996$), $I_{UA}=0.26v+6.43$ ($R^2=0.9996$), respectively. The results indicate the typical surface-controlled process. The results show that AA, DA and UA can easily adsorb onto the electrode surface, and thus there was sufficient time for their oxidation.

3.4 Individual determination of AA, DA and UA on RGO/PDA/Au nanocatalyst

The individual determination of AA, DA and UA at the RGO/PDA/Au/GCE are performed by differential pulse voltammetry (DPV) experiment.

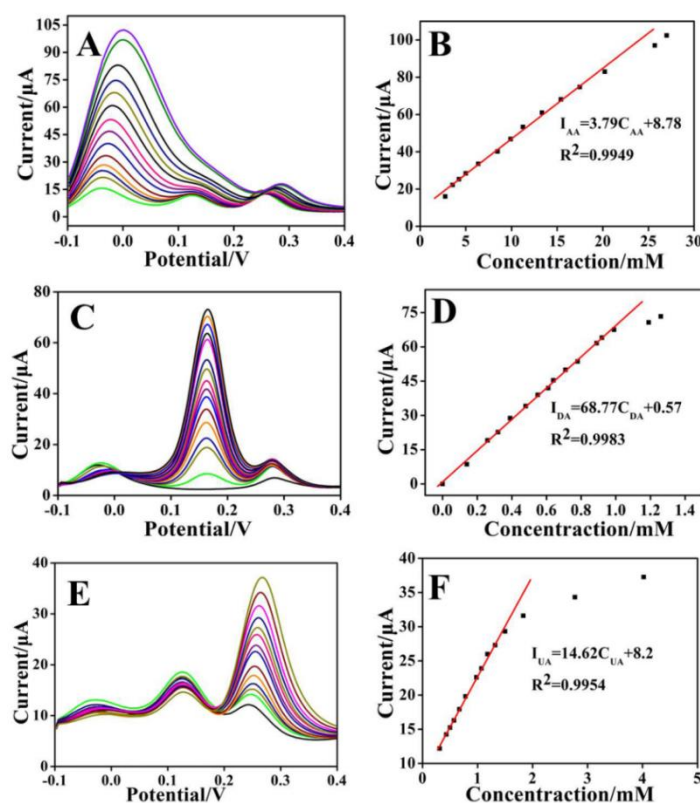


Figure 6. (A) DPV of AA at the RGO/PDA/Au/GCE in the presence of 0.28 mM DA and 0.69 mM UA, AA concentrations: 2.84, 3.55, 4.25, 5.00, 6.36, 8.47, 9.9, 11.26, 13.34, 15.42, 17.48, 18.11, 20.22, 25.70, and 27.01 mM; (B) the linear relationship between currents and AA concentration; (C) DPV of DA at the RGO/PDA/Au/GCE in the presence of 0.14 mM AA and 0.29 mM UA, DA concentrations: 0, 0.14, 0.21, 0.28, 0.35, 0.42, 0.50, 0.57, 0.64, 0.71, 0.78, 0.85, 0.92, 0.99, 1.19, 1.26, and 1.33 mM; (D) the linear relationship between currents and DA concentration; (E) DPV of UA at the RGO/PDA/Au/GCE in the presence of 0.36 mM AA and 0.29 mM DA, UA concentrations: 0.29, 0.36, 0.43, 0.50, 0.71, 0.78, 0.93, 1.00, 1.07, 1.21, 1.34, 1.54, 2.50, and 4.36 mM; (F) the linear relationship between currents and UA concentration. Supporting electrolyte: 0.2 M PBS (pH 7.0).

Only concentration of target analyte was increased while the concentrations of the other two species were kept constant in PBS. As shown in Figure 6, the electrochemical response of AA, DA and UA increase linearly with the increase of the target analyte concentrations. And the oxidation peaks potentials of AA, DA and UA are -0.03, 0.16 and 0.26 V, respectively. For AA, the linear regression equation is calibrated as $I_{AA}=3.79 C_{AA}+8.78$ (C_{AA} : 2.84-27.01 mM) and the R^2 is 0.9949. For DA, the linear regression equation is calibrated as $I_{DA}=68.77 C_{DA}+0.57$ (C_{DA} : 0-1.33 mM) and the R^2 is 0.9983. For UA, the linear regression equation is calibrated as $I_{UA}=14.62 C_{UA}+8.2$ (C_{UA} : 0.29-4.36 mM) and the R^2 is 0.9954. It is also found that addition of the target analytes into the electrochemical cell does not have significant influence on the peak currents and peak potentials of the other two biomolecules. These results show that the fabricated RGO/PDA/Au/GCE sensor can efficient separate and determine the AA, DA and UA. It is noted that no interference between each other in the measurements.

3.5 Simultaneous determination of AA, DA and UA on RGO/PDA/Au nanocatalyst

Simultaneous determination of AA, DA and UA is carried out on RGO/PDA/Au/GCE by the simultaneously increasing the concentrations of the three analyte. The electrochemical response of AA, DA and UA still increases linearly with the increase of their concentrations (Figure 7).

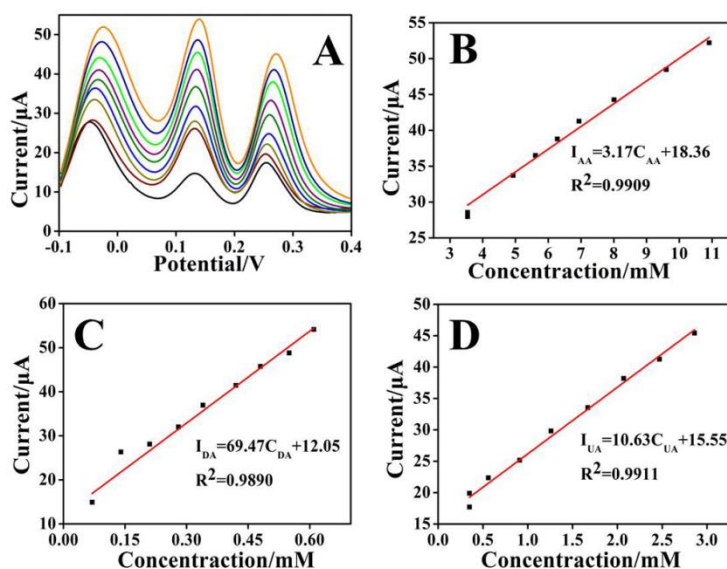


Figure 7. (A) DPV profiles at RGO/PDA/Au/GCE in 0.2 M PBS (pH 7.0) containing different concentrations of AA, DA and UA. From bottom to up the concentrations from 3.54 to 10.91 mM for AA, 0.14 to 0.61 mM for DA and 0.35 to 2.86 mM for UA, respectively. (B)-(D) Plots of the oxidation peak currents as a function of AA, DA and UA concentrations, respectively.

The linear equation of AA can be described as $I_{AA} = 3.17 C_{AA}+18.36$ ($R^2 = 0.9909$) with the linearity range of 4.93-9.60 mM. For DA, the linear equation is $I_{DA} = 69.47 C_{DA}+12.05$ ($R^2 = 0.9890$) with the linearity range of 0.34 mM-0.61 mM. While for UA the linear relationship is $I_{UA} = 10.63$

$C_{UA}+15.55$ ($R^2 = 0.9911$) with the linearity range of 0.38 mM -2.86 mM. The detection limits are 1.64 mM, 0.11 mM, 0.13 mM (S/N=3) for AA, DA and UA, respectively. The results prove that the fabricated RGO/PDA/Au/GCE sensor with good electrocatalytic activity can be used to individual and simultaneous determination of AA, DA and UA. That will be contributed to the PDA successfully functionalized graphene. RGO/PDA nanocomposites possess a large surface area can adsorb high density of Au NPs. Au NPs possess unique biocompatibility and excellent conductivity can absorb a large amount of molecules on the Au NPs active centers. That will benefit for the electrocatalytic oxidation of AA, DA and UA [21].

4. CONCLUSION

In summary, Au NPs decorated RGO/PDA nanocomposites were obtained by a simple and green method. Then the electrochemical sensor was fabricated for determination of AA, DA, and UA based on RGO/PDA/Au/GCE. The fabricated sensor not only detected individually but also well separated each other while detecting simultaneously three compounds. The detection limit of AA, DA and UA are 1.64 mM, 0.11 mM, 0.13 mM, respectively. The results further prove that the prepared RGO/PDA/Au nanocatalyst possesses an excellent electrocatalytic oxidation of AA, DA and UA. This work may provide a valuable clue for the use of graphene based nanomaterials to detect electroactive biomolecules.

ACKNOWLEDGEMENTS

This work was supported by the National Natural Science Foundation of China (No. 21665008), Youth project of Yunnan Province (No 2014FD054), the Scientific Research Fund Project of Honghe University (XJ14Z02), Young and Middle-aged Academic and Reserve Program (2018HB005), the Doctor Start-up Fund of Honghe University (XJ16B04), Honghe University Young Academic Reserve Program (2016HB0401), the Yunnan education department of Scientific Research Foundation (2018JS478).

References

1. W. J. Zhang, L. Liu, Y. G. Li, D. Y. Wang, H. Ma, H. L. Ren, Y. L. Shi, Y. J. Han and B. C. Ye, *Biosensors and Bioelectronics*, 121 (2018) 96.
2. N. M. M. A. Edris, J. Abdullah, S. Kamaruzaman, M. I. Saiman and Y. Sulaiman, *Arabian Journal of Chemistry*, 11 (2018) 1301.
3. W. Sroysee, S. Chairam, M. Amatatongchai, P. Jarujamrus, S. Tamuang, S. Pimmongkol, L. Chaicharoenwimolkul and E. Somsook, *Journal of Saudi Chemical Society*, 22 (2018) 173.
4. N. Tukimin, J. Abdullah and Y. Sulaiman, *J. Electrochem. Soc.*, 165 (2018) B258.
5. H. Ibrahim and Y. Temerk, *J. Electroanal. Chem.*, 780 (2016) 176.
6. M. He, G. Fei, Z. Zheng, Z. Cheng, Z. Wang and H. Xia, *Langmuir*, 10.1021/acs.langmuir.9b00021 (2019).
7. X. C. Liu, G. C. Wang, R. P. Liang, L. Shi and J. D. Qiu, *J. Mater. Chem. A*, 1 (2013) 3945.
8. H. Lee, S. M. Dellatore, W. M. Miller and P. B. Messersmith, *Science*, 318 (2007) 426.
9. J. J. Zhou, C. X. Wang, P. Wang, P. B. Messersmith and H. W. Duan, *Chem. Mater.*, 27 (2015) 3071.

10. C. Q. Ruan, W. Shi, H. R. Jiang, Y. N. Sun, X. Liu, X. Y. Zhang, Z. Sun, L. F. Dai and D. T. Ge, *Sensors and Actuators B*, 177 (2013) 826.
11. F. F. Ren, C. Y. Zhai, M. S. Zhu, C. Q. Wang, H. W. Wang, D. Bin, J. Guo, P. Yang and Y. K. Du, *Electrochimica Acta*, 153 (2015) 175.
12. W. S. Hummers and R. E. Offeman, *J. Am. Chem. Soc.*, 80 (1958) 1339.
13. Y. Si and E. T. Samulski, *Nano Lett.*, 8 (2008) 1679.
14. Z. F. Wang, G. Z. Gou, L. Shi, J. Yang, C. Xu, L. Zhang, A. P. Fan and Y. Min, *J. Appl. Polym. Sci.*, (2018) 46720.
15. Y. Luo, F. Y. Kong, C. Li, J. J. Shi, W. X. Lv and W. Wang, *Sensor Actuat. B-Chem*, 234 (2016) 625.
16. S. Li, S. Guo, H. Yang, G. Gou, R. Ren, J. Li, Z. Dong, J. Jin and J. Ma, *J. Hazard. Mater.*, 270 (2014) 11.
17. P. Yu, J. Zhang, T. Zheng and T. Wang, *Colloid. Surface A*, 494 (2016) 241.
18. R. Devasenathipathy, V. Mani, S. Chen, D. Arulraj and V. S. Vasantha, *Electrochim. Acta*, 135 (2014) 260.
19. M. L. Liu, Q. Chen, C. L. Lai, Y. Y. Zhang, J. H. Deng, H. T. Li and S. Z. Yao, *Biosensors and Bioelectronics* 48 (2013) 75.
20. H. Yang, J. Zhao, M. J. Qiu, P. Sun, D. X. Han, L. Niu and G. F. Cui, *Biosensors and Bioelectronic*, (2019).
21. Q. Zhu, J. Bao, D. Q. Huo, M. Yang, C. J. Hou, J. F. Guo, M. Chen, H. B. Fa, X. G. Luo and Y. Ma, *Sensors and Actuators B*, 238 (2017) 1316.